Anti-glioblastoma efficacy and safety of paclitaxel-loading Angiopep-conjugated dual targeting PEG-PCL nanoparticles

Hongliang Xin [a,b], Xianyi Sha [a], Xinyi Jiang [a], Wei Zhang [a], Liangcen Chen [a], Xiaoling Fang [a,*]

[a] Key Laboratory of Smart Drug Delivery, Ministry of Education & PLA, School of Pharmacy, Fudan University, Lane 826, Zhangheng Road, Shanghai 201203, China
[b] Department of Pharmaceutics, School of Pharmacy, Nanjing Medical University, Nanjing 210029, China

ARTICLE INFO

ABSTRACT

Therapeutic effect of glioma is often limited due to low permeability of delivery systems across the Blood-Brain Barrier (BBB) and poor penetration into the tumor tissue. In order to overcome the two barriers, we proposed Angiopep-conjugated PEG-PCL nanoparticles (ANG-PEG-NP) as a dual targeting drug delivery system for glioma treatment basing on low density lipoprotein receptor related protein (LRP) receptor not only over-expressed on BBB but also on glioma cells. This system could transport across BBB through LRP-mediated transcytosis and then targeted glioma via LRP-mediated endocytosis. In this study, we evaluated the preliminary availability and safety of ANG-PEG-NP for glioma treatment. The penetration, distribution, and accumulation into 3D glioma spheroid and in vivo glioma region of ANG-PEG-NP were obviously higher than that of plain PEG-PCL nanoparticles (PEG-NP). The anti-glioblastoma efficacy of paclitaxel (PTX) loading ANG-PEG-NP was significantly enhanced as compared to that of Taxol and PEG-NP. Preliminary safety results showed that no acute toxicity to hematological system, liver, kidney and brain tissue was observed after intravenous administration with a dose of 100 mg/kg blank ANG-PEG-NP per day for a week. Results indicate that Angiopep-conjugated dual targeting PEG-PCL nanoparticle is a potential brain targeting drug delivery system for glioma treatment.

© 2012 Elsevier Ltd. All rights reserved.

1. Introduction

At present, glioblastoma multiforme (GBM) is the most frequent primary central nervous system tumor in human. Although the advances in other solid tumor therapy have improved the survival of patients, GBM prognosis is still poor, with a 14-month median survival time despite interventions [1]. Because GBM is different from other cancers by its diffuse invasion of the surrounding normal brain tissue, it is impossible to make the complete removal of glioma by conventional surgery and the chances of glioma recurrence from residual tumors are very high [2]. Therefore, chemotherapy is indispensable for glioma treatment after the surgery [3]. Unfortunately, the GMB treatment by chemotherapy is very limited due to the rare blood brain barrier (BBB) penetration and poor glioma targeting of the chemotherapeutics [4]. Although compromised endothelial barrier which facilitates molecular transport under glioma condition exists [5,6], BBB still plays important role in the infiltrating margin of glioma and should be considered for glioma treatment and diagnosis [7]. Paclitaxel (PTX)

is a new class of microtubule stabilizing agents with perfect anti-glioma activity [8,9]. However, the activity of commercial PTX preparation against glioblastoma has been disappointing in clinical study because of drug-resistance and poor penetration across the BBB [10,11]. Accordingly, it is impending to develop a targeted drug delivery system with high BBB penetration and glioma targeting abilities.

To overcome BBB and blood tumor barrier (BTB) [12,13], dual targeting drug delivery systems based on receptor-mediated endocytosis were developed to deliver chemotherapeutic agent across BBB and simultaneously target brain tumor [14]. The most common dual targeting strategy is based on modification of nanocarriers with two kinds of ligands, one of which can target to BBB, the other can target to glioma cancerous cells [15,16]. It has been reported that low density lipoprotein receptor related protein (LRP) is not only over-expressed on BBB but also on glioma cancerous cells. Thus, another dual targeting strategy was developed to decorate the surface of nanocarriers with one single ligand [17]. In our previous study, Angiopep-2, a specific ligand of LRP receptor, was used to modify poly(-ethylene glycol)-co-poly(ε-caprolactone) (PEG-PCL) copolymer nanoparticles to develop a dual targeting drug delivery system (ANG-PEG-NP) for PTX delivery [17]. The glioma dual targeting

* Corresponding author. Tel.: +86 21 51980071; fax: +86 21 51980072.
E-mail address: xlfang@shmu.edu.cn (X. Fang).

strategy of PTX loading Angiopep-conjugated PEG-PCL nano-particles (ANG-PEG-NP-PTX) was shown as Fig. 1, which denoted that Angiopep-2 mediated transcytosis of ANG-PEG-NP-PTX across BBB through LRP as grade I targeting, followed by endocytosis of ANG-PEG-NP-PTX via recognition of LRP on the surface of glioma cells as grade II targeting. The *in vitro* and *in vivo* brain targeting mechanism [18] and enhancement of cytotoxicity to U87 MG glioma cells [17] of ANG-PEG-NP were also confirmed in our previous studies. However, there are still several challenges need to be addressed: firstly, since the solid tumor microenvironment which contains clusters of tumor cells, nonuniform leaky vasculature and a dense interstitial structure differs from *in vitro* cancerous cells by its structural heterogeneity [19], so can ANG-PEG-NP enhance the penetration, distribution, and accumulation of chemotherapeutic agent in the solid tumor *in vivo*? Secondly, what will be the difference between targeted and non-targeted nanoparticles in anti-glioblastoma efficacy assessment using intracranial glioma mice model? Thirdly, considering part of ANG-PEG-NP will accumulate in the brain parenchyma and other organ tissues, can this accumulation of dual targeting nanoparticles induce functional disorder and other toxicities?

In this study, we used *ex vivo* 3D glioma tumor spheroids and intracranial glioma mice model to evaluate the penetration, distribution, and accumulation of ANG-PEG-NP into brain tumor. The *in vivo* anti-glioblastoma efficacy of ANG-PEG-NP was investigated by intracranial glioma mice model as well. The safety of ANG-PEG-NP following intravenous injection was carried out using healthy mice.

2. Materials and methods

2.1. Materials

Methoxyl poly(ethylene glycol)-co-poly(ε-caprolactone) copolymer (Me-PEG–PCL, 12 KDa) and Maleimidyl-poly(ethylene glycol)-co-poly(ε-caprolactone) copolymer (Maleimide-PEG-PCL, 14 KDa) were synthesized by the ring opening polymerization as described before [17]. Rhodamine B isothiocyanate (RBITC), Propidium Iodide (PI), MTT were purchased from Sigma (St. Louis, MO, USA). Low melting-point agarose was obtained from Yixin Biotechnology Co., Ltd. (Shanghai, China). Angiopep (TFFYGGSRGKRNNFKTEEYC) was synthesized by Shanghai Gene-Pharma Co., Ltd Company (Shanghai, China). Penicillin-streptomycin, DMEM, fetal bovine serum (FBS) and 0.25% (w/v) trypsin solution were purchased from Gibco BRL (Gaithersberg, MD, USA). BCA kit and TritonX-100 were purchased from Beyotime Biotechnology Co., Ltd. (Nantong, China). All the other solvents were analytical grade.

2.2. Cell line

The U87 MG cell line was obtained from Institute of Biochemistry and Cell Biology, Shanghai Institutes for Biological Sciences, Chinese Academy of Sciences (Shanghai, China). Brain capillary endothelial cells (BCECs) were kindly provided by Prof. X. G. Jiang (School of Pharmacy, Fudan University). Both cell lines were cultured in DMEM medium, supplemented with 10% FBS, 1% nonessential amino acids, 100 IU/mL penicillin and 100 μg/mL streptomycin sulfate. Cells were cultured in incubators maintained at 37 °C with 5% CO_2 under fully humidified conditions. All experiments were performed in the logarithmic phase of cell growth.

2.3. Animals

Male BALB/c nude mice and ICR mice, aging 4—5 weeks and weighing 20 ± 2 g, were supplied by Department of Experimental Animals, Fudan University (Shanghai, China). Mice were acclimated at 25 °C and 55% of humidity under natural light/dark conditions for 1 week before animal study. All animal experiments were carried out in accordance with the guidelines approved by the ethics committee of Fudan University (Shanghai, China).
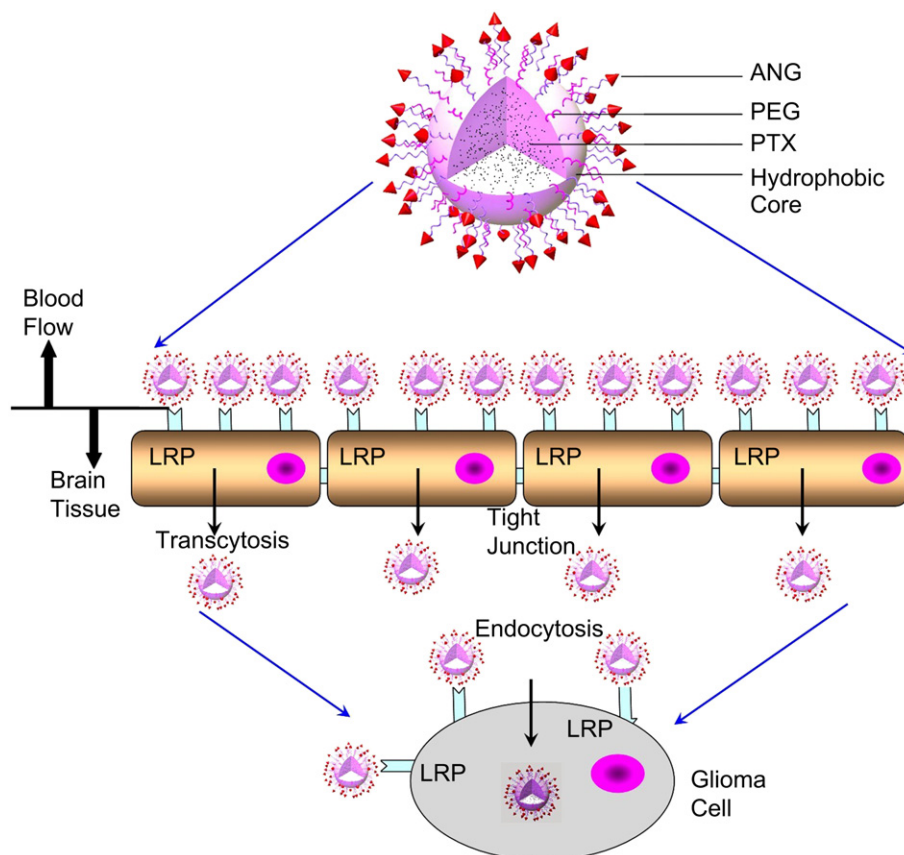

Fig. 1. Design of PTX loading Angiopep-conjugated polymer nanoparticles as dual targeting drug delivery system for glioma via LRP mediated endocytosis.

2.4. Preparation and characterization of ANG-PEG-NP

ANG-PEG-NP-PTX and RBITC labeled ANG-PEG-NP were prepared as previously reported [17,18]. The particle size distribution of the dual targeting nanoparticles was measured by the light scattering method using a Nicomp Zeta Potential/Particle Size (model 380XLS, NicompTM, Santa Barbara, CA, USA). The PTX loading coefficient (DL%) and encapsulation ratio (ER%) were measured by HPLC as previously described [20].

2.5. Avascular human glioma tumor spheroids

The ex vitro 3D glioma tumor spheroids of U87 MG cells were developed using liquid overlay system [21,22]. Agarose solution was prepared in serum free DMEM (2% w/v) by heating it at 80 °C for 30 min. Each well of 96-cell culture plates was coated with a thin layer (80 μL) of sterilized agarose-based DMEM. Tumor cells were seeded into each well at the density of 2000 cells/well (in complete medium). Subsequently, plates were gently agitated for 5 min on the first day of seeding and tumor spheroids were allowed to grow for 7 days at 37 °C in the presence of 5% CO_2. Cell culture medium was changed every 2 days. The uniform and compact tumor spheroids were selected for the follow-up studies.

2.6. Diffusion of dual targeting nanoparticles into the glioma spheroids

Tumor spheroids were incubated with RBITC labeled nanoparticles (500 μg/mL) for 24 h. After incubation, tumor spheroids were washed four times with ice cold PBS, fixed with formaldehyde (10% w/v in PBS) for 30 min, and placed in cavity microscope slides. The center of the spheroids microscope images were acquired by tomoscan using confocal laser scanning microscopy (Leica TCS SP5, Germany).

2.7. Determination of cell viability in the glioma spheroids

Propidium iodide was used as fluorescent probe to distinguish the dead cells in the glioma spheroids after treatment with PTX formulations. Therefore, the U87 MG glioma spheroids were incubated with DMEM, Taxol, PEG-NP-PTX and ANG-PEG-NP-PTX for 7 days, respectively. Subsequently, the glioma spheroids were incubated with propidium iodide (50 μg/mL) for 30 min at 4 °C. After incubation, the glioma spheroids were washed four times with ice cold PBS and lysed with 0.5% Triton-X. Fluorescence in the cell lysate was measured by using Safire plate reader (TECAN M1000, Switzerland). Protein content of tumor spheroids was measured using micro BCA kit.

2.8. Growth inhibition of the glioma spheroids

The U87 MG glioma spheroids were incubated with DMEM, Taxol, PEG-NP-PTX and ANG-PEG-NP-PTX, respectively. Samples were added per well to obtain a concentration of 0.5−1 μg/mL. Growth inhibition was monitored by measuring the size of the U87 MG glioma spheroids using an inverted phase microscope fitted with an ocular micrometer each day. The major (d_{max}) and minor (d_{min}) diameter of each spheroid was determined and spheroid volume was calculated as previously mentioned [23,24] by using the following formula: $V = (\pi \times d_{max} \times d_{min})/6$. The U87 MG glioma spheroids volume ratio was calculated with the formula: $R = (V_{day\ i}/V_{day\ 0}) \times 100\%$, where $V_{day\ i}$ is the U87 MG glioma spheroids volume at the ith day after treatment, and $V_{day\ 0}$ is the U87 MG glioma spheroids volume prior to administration.

2.9. In vivo glioma distribution

The orthotope glioma tumor bearing mice model was established as reported [17]. Briefly, U87 MG cells (1.0×10^5 cells suspended in 5 μL PBS) were implanted into the right striatum (1.8 mm lateral to the bregma and 3 mm of depth) of nude mice using a stereotactic fixation device with mouse adapter. Ten days after implantation, the mice were administered with RBITC labeled PEG-NP and ANG-PEG-NP via the tail vein at a dose of 100 mg/kg, respectively. Animals were anesthetized with diethyl ether 2 h post administration. Then, ventricular perfusion was conducted with saline and 4% paraformaldehyde for 30 min, respectively. Subsequently, the brain tissues were harvested, fixed in 4% paraformaldehyde for 24 h, placed in 15% sucrose PB solution for 24 h until subsidence, then in 30% sucrose for 24 h until subsidence. Afterwards, brain tissues were frozen in O.C.T. embedding medium at −80 °C. Frozen sections with 20 μm thickness were prepared with a cryotome Cryostat (Leica, CM 1900, Wetzlar, Germany) and stained with 1 μg/mL DAPI for 10 min at room temperature. After washing twice with PBS (pH 7.4), the sections were immediately examined under the fluorescence microscope (Leica DMI 4000B, Germany).

2.10. In vivo anti-glioma efficacy

The in-vivo anti-glioma efficacy of PTX loading dual targeting nanoparticles was evaluated by orthotope glioma bearing mice model. Three days after glioma inoculation, the glioma bearing nude mice were randomly divided into four groups (10 mice per group). Three groups of the mice were treated with 100 μL of Taxol, PEG-NP-PTX and ANG-PEG-NP-PTX at a dose of 10 mg/kg PTX every three days with total 3 doses, respectively. Another group was administrated with physiological saline as blank control. At day 14, three mice of each group were sacrificed for measuring the tumor size, and other seven mice were used for monitoring the survival curves [25]. The brain tissue was collected and fixed in formalin, glioma volume was determined with a vernier caliper. The tumor volume was estimated using the formula: Volume = length × width × height, and the inhibition ratio of tumor (%) was calculated with the formula: IRT = $[(V_{control} − V_{drug})/V_{control}] \times 100\%$, where V_{drug} is the glioma volume after treatment, and $V_{control}$ is the glioma volume of physiological saline group. The glioma was fixed with paraformaldehyde for 48 h and embedded in paraffin. Each section was cut into 5 μm, processed for routine hematoxylin and eosin (H&E) staining, and then visualized under fluorescent microscope (Leica DMI 4000B, Germany). The survival time was calculated from day 0 since tumor inoculation to the day of death. Kaplan−Meier survival curves were plotted for each group.

2.11. Cytotoxicity assay

The cytotoxicity of the ANG-PEG-NP was evaluated in BCECs and U87 MG. Following three days of continuous exposure to the ANG-PEG-NP, cell viability was measured using MTT assay. The absorbance was measured using a microplate reader (Thermo Multiskan MK3, USA), with a test wavelength of 570 nm and a reference wavelength of 630 nm. The percentage of viable cells at each concentration relative to that of non-treated cells was plotted as a function of PTX concentration. Blank PEG-NP and Angiopep were used as controls, respectively.

2.12. In vivo safety evaluation

Sixteen male ICR mice were randomly divided into two groups ($n = 8$). Each group received an intravenous injection of blank ANG-PEG-NP (100 mg/kg) or saline at one dose per day for a week. The body weight was monitored each day. Blood sample and brain tissue were collected at 24 h after the last administration for hematologic and histochemistry analysis. White blood cell (WBC), red blood cell (RBC) and platelet (PLT) were measured by Advia 120 Automated Hematology Analyzer (Bayer Ltd., Germen). The serum aspartate transanimase (AST), alanine transaminase (ALT), total bilirubin (TBIL), ureanitrogen (BUN) and creatinine levels were assayed using Hitachi 7080 Chemistry Analyzer (Hitachi Ltd., Japan). The brain tissue was fixed with paraformaldehyde for 48 h and embedded in paraffin. Each section was cut into 5 μm, processed for routine hematoxylin and eosin (H&E) staining, and then visualized under fluorescent microscope (Leica DMI 4000B, Germany).

3. Results and discussion

3.1. Preparation and characterization of ANG-PEG-NP

In the process of nanoparticle fabrication, about 10% Me-PEG-PCL copolymer was replaced by Maleimide-PEG-PCL copolymer which can specifically react with the thiol group of Angiopep. The average particle size of ANG-PEG-NP was about 90 nm, which may accumulate more readily in tumor due to the Enhanced Permeability and Retention (EPR) effect [26,27]. The PTX loading coefficient and encapsulation ratio of ANG-PEG-NP were about 7% and 86%, respectively. To trace the nanoparticles qualitatively, RBITC was used as fluorescent probe to label nanoparticles through conjugation with PEG-PCL copolymer via covalent coupling [18].

3.2. Diffusion of dual targeting nanoparticles into the glioma spheroids

It was reported that therapeutic drug accessing inside the solid tumors is limited because of the poor permeation of drug delivery systems into the hypoxic and necrotic tumor regions distant from the vascular bed [28,29]. Therefore, the chemotherapeutic efficacy of drug is compromised, inducing the recurrence of cancer. The poor permeation of drug delivery system is particularly serious in malignant glioma which is one of the most refractory tumors [30]. Enhancement of the drug delivery system to penetrate deeper into the glioma tissues can significantly reduce the further glioma growth and augment the therapeutic effect of the treatment [24]. The ex vivo 3D tumor spheroids generated by liquid overlay technique are not only aggregates of cells in close contact but contain an

organized extracellular matrix consisting of fibronectin, laminin, collagen, and GAG, suggestive of the extracellular matrix of tumors *in vivo* [31]. Thereby 3D multicellular model has become the most commonly used tool to evaluate the effect of drug delivery system on the penetration into tumor tissues [32,33]. In this study, we constructed the U87 MG glioma *ex vivo* 3D tumor spheroids by liquid overlay technique. After 7 days culture, the glioma spheroids became compact and homogeneous (Fig. 2A and B). Confocal laser scanning microscopic imaging of glioma spheroids showed that PEG-NP was present only in the periphery after 24 h of incubation; however, the rate and extent of diffusion were greater in ANG-PEG-NP group (Fig. 2C and D). It suggested that the permeation ability into glioma of ANG-PEG-NP was obviously greater than that of unmodified nanoparticles, which might due to LRP mediated endocytosis.

3.3. Cell viability in the glioma spheroids

Propidium iodide can stain the DNA of dead cells selectively, and thus, its fluorescence intensity relates to dead cell population [34]. Thereby we used propidium iodide as a fluorescent probe for determining the dead cells in the glioma spheroids after treatment with PTX formulations. As presented in Fig. 3, the fluorescence intensity of propidium iodide in the glioma spheroids treated with DMEM, Taxol, PEG-NP-PTX and ANG-PEG-NP-PTX was 3.4×10^5/(mg protein), 1.2×10^6/(mg protein), 1.4×10^6/(mg protein) and 2.4×10^6/(mg protein), respectively, suggesting that ANG-PEG-NP can induce a statistically significant increase in cell death of the glioma spheroids as compared to the Taxol and plain nanoparticles
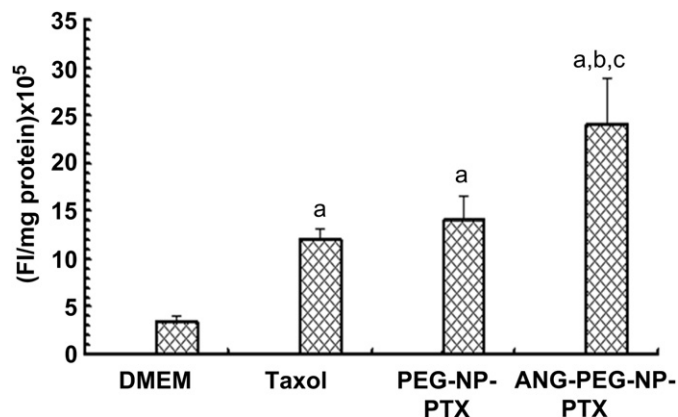

Fig. 3. Accumulation of PI in U 87 MG tumor spheroids subjected to different treatments. PI stains the DNA of dead cells, and thus, its fluorescence intensity relates to dead cell population. Data are mean values + SD. a, Statistically significant difference with respect to blank DMEM ($p < 0.05$, one-way ANOVA); b, Statistically significant difference with respect to Taxol ($p < 0.05$, one-way ANOVA); c, Statistically significant difference with respect to PEG-NP-PTX ($p < 0.05$, one-way ANOVA).

($p < 0.05$, one-way ANOVA), which maybe due to the active targeting of ANG-PEG-NP via LRP mediated endocytosis.

3.4. Growth inhibition of the glioma spheroids

The influence of various treatments on the growth of glioma spheroids was also investigated in this study. Fig. 4 represented
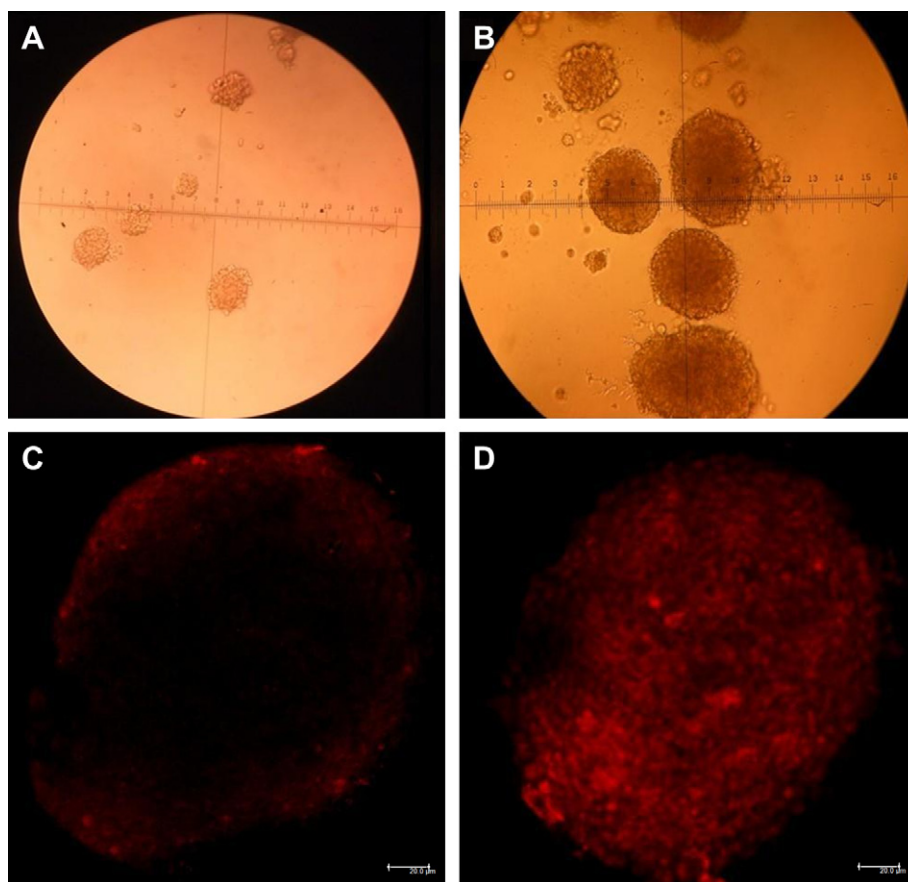

Fig. 2. The U87 MG tumor spheroids at day 3 (A) and day 7 (B) after cells seeded, images were acquired at 10×. Confocal microscope images of U87 MG tumor spheroids incubated with RBITC labeled PEG-NP (C) and ANG-PEG-NP (D) for 24 h. Bar: 20 μm.
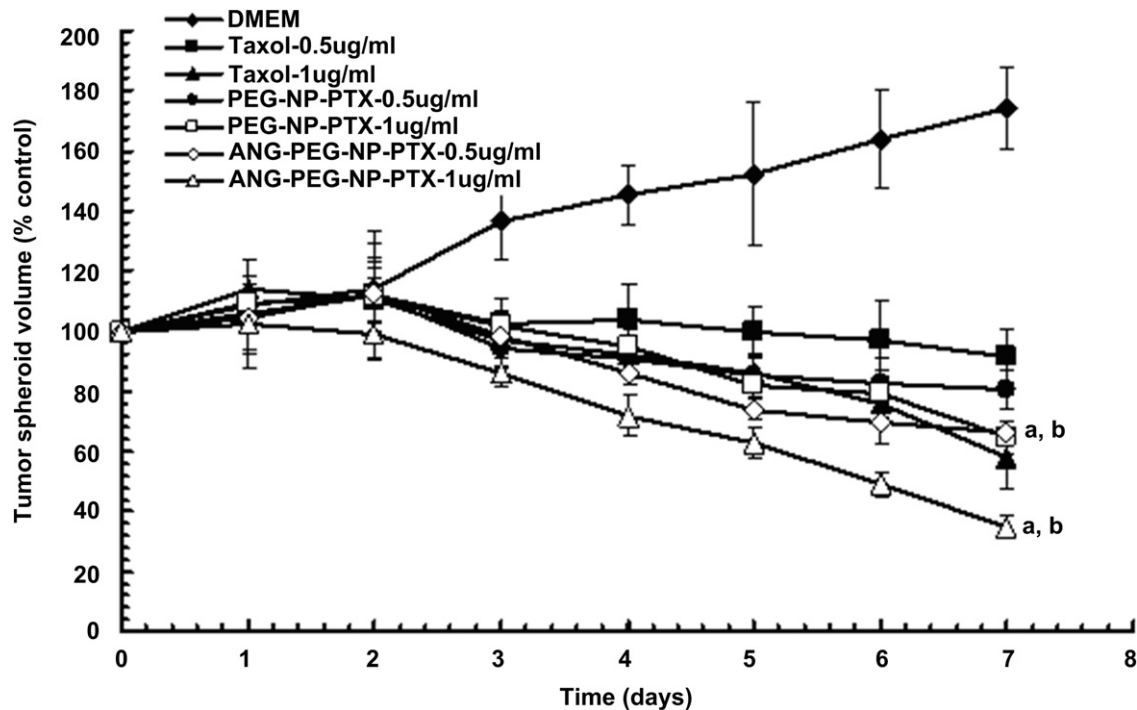
Fig. 4. Inhibition in the growth of U87 MG tumor spheroids on treatment with Taxol or PTX-loading nanoparticles at different concentration of PTX. The diameter of tumor spheroids was measured using a microscope fitted with an ocular micrometer, and the volume of the spheroids was calculated. Data are mean values ± SD. a, Statistically significant difference with respect to Taxol ($p < 0.01$). b, Statistically significant difference with respect to PEG-NP-PTX ($p < 0.01$).

that the U87 MG glioma spheroid volume ratios after treatment of Taxol, PEG-NP-PTX and ANG-PEG-NP-PTX at different PTX concentration, respectively. It was observed that glioma spheroids continued to grow in volume in the absence of any drug (174% of the control after 7 days). The obvious reduction in volume of U87 MG glioma spheroids was observed for all PTX preparations after 7 days treatment, indicating that U87 MG

glioma spheroids were sensitive to PTX. The U87 MG glioma spheroid volume ratio was 91.3%, 80.4% and 66.4% at 0.5 μg/mL and 58.1%, 64.9% and 35.2% at 1.0 μg/mL for Taxol, PEG-NP-PTX and ANG-PEG-NP-PTX, respectively. Results showed that ANG-PEG-NP significantly improves the inhibitory effects on the 3D glioma spheroids. Since the tumor spheroid mimics the micro-environment of *in vivo* glioma solid tumor, the higher inhibitory
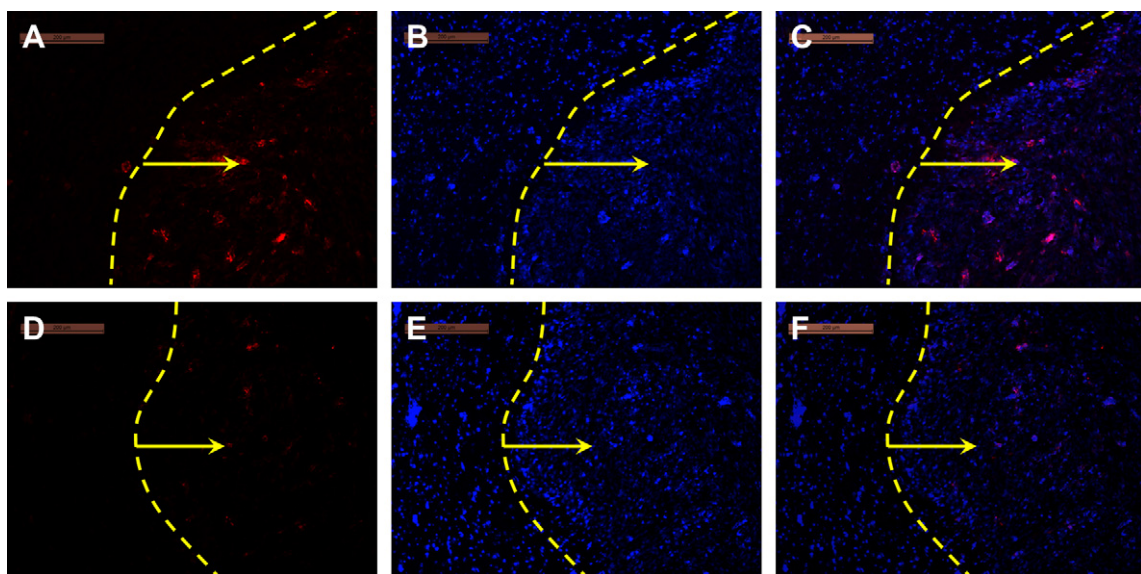

Fig. 5. *In vivo* glioma distribution of RBITC labeled nanoparticles in the brains of orthotope glioma mice treated with RBITC labeled ANG-PEG-NP (A–C) and RBITC labeled PEG-NP (D–F) 120 min after intravenous administration. Image C is the combination of A and B; image F is the combination of D and E; frozen sections (20 μm of thickness) of glioma were examined by fluorescent microscopy. Red: RBITC. Blue: cell nuclei. Yellow line: border of the glioma. Yellow arrow: direction of the glioma. Bar: 200 μm. (For interpretation of the references to colour in this figure legend, the reader is referred to the web version of this article.)

effect suggests that ANG-PEG-NP-PTX may improve therapeutic effect *in vivo*.

3.5. In vivo glioma distribution

The *in vivo* glioma distribution and targeting capability of RBITC labeled ANG-PEG-NP was studied qualitatively by fluorescence microscopic observation of coronal sections of the orthotope glioma bearing mouse brain. Results showed that there was only a slight red particles of RBITC labeled PEG-NP distributed in glioma region due to EPR effect (Fig. 5D–F), but a significantly higher distribution of the RBITC labeled ANG-PEG-NP in the glioma was observed (Fig. 5A–C). Because of the equal contribution of EPR effect for PEG-NP group and ANG-PEG-NP group, the enhancement of penetration and distribution in glioma region of ANG-PEG-NP might result from the BBB

penetration improvement via LRP-mediated transcytosis. Meanwhile, the fluorescence of RBITC labeled ANG-PEG-NP was almost undetectable in the normal brain tissue, which suggested Angiopep-2 modification could facilitate enrichment of nanoparticles in glioma selectively. It was found that ANG-PEG-NP could facilitate the transportation across the BBB and then enhance the penetration, distribution, and accumulation of chemotherapeutic agent in the solid glioma.

3.6. In vivo anti-glioma efficacy

The *in vivo* antitumor efficiency of Taxol, PEG-NP-PTX and ANG-PEG-NP-PTX was validated in the orthotope U87 MG glioma-bearing mice. As shown in Fig. 6A, after treated with saline, Taxol, PEG-NP-PTX and ANG-PEG-NP-PTX, the glioma tumor volume was 55.72 mm^3, 44.29 mm^3, 35.59 mm^3 and 19.35 mm^3 at day 14,
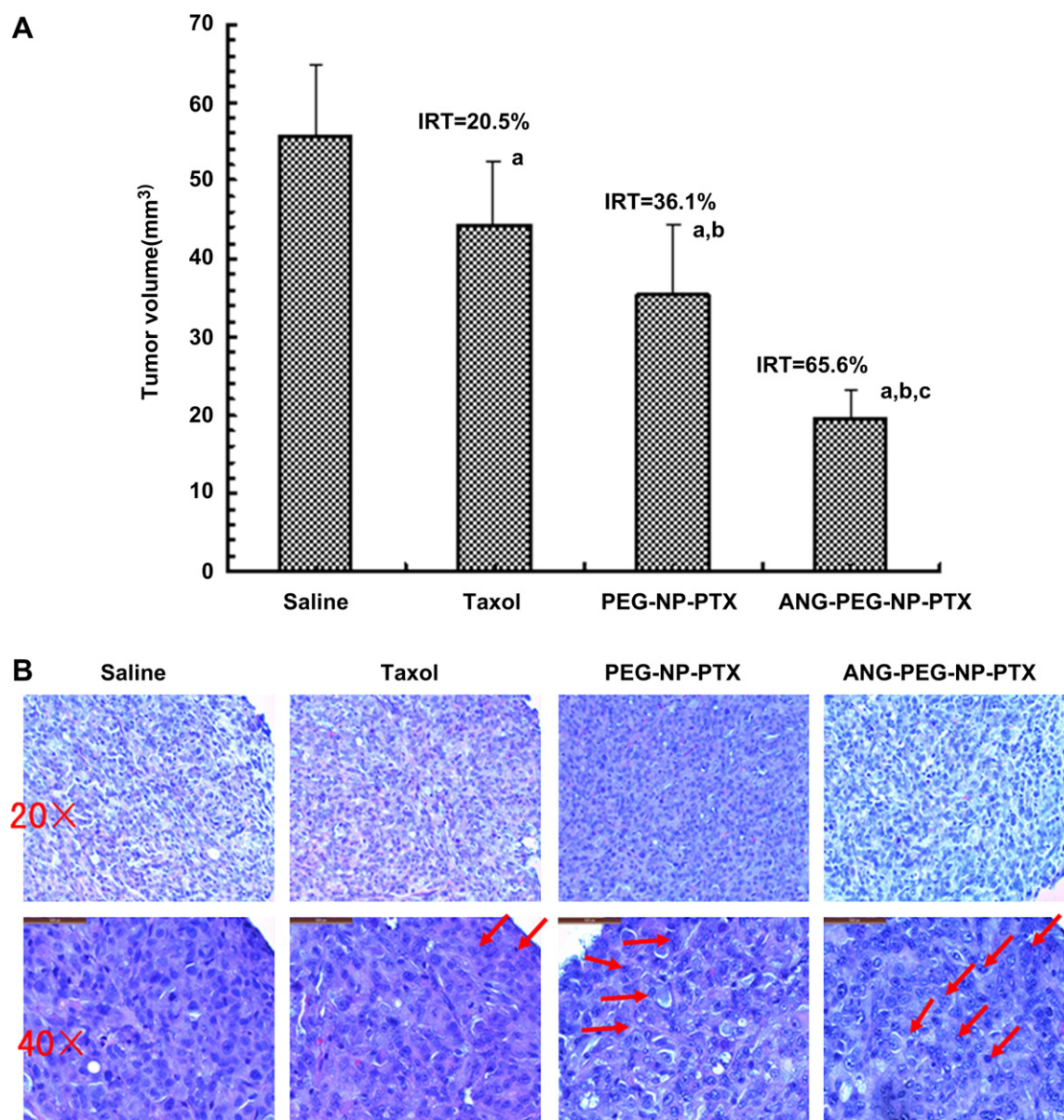

Fig. 6. The glioma tumor volume of each treatment group at the time of sacrifice. IRT: inhibition ratio of tumor (%) a, $p < 0.05$, compared with saline; b, $p < 0.05$, compared with Taxol; c, $p < 0.05$, compared with PEG-NP-PTX ($n = 3$) (A); tumor sections (thickness of 20 μm) were examined by fluorescence microscopy after stained with hematoxylin and eosin for histopathological analysis, red arrow: position of the apoptotic nuclei, original magnification: ×20 or ×40 (B). (For interpretation of the references to colour in this figure legend, the reader is referred to the web version of this article.)
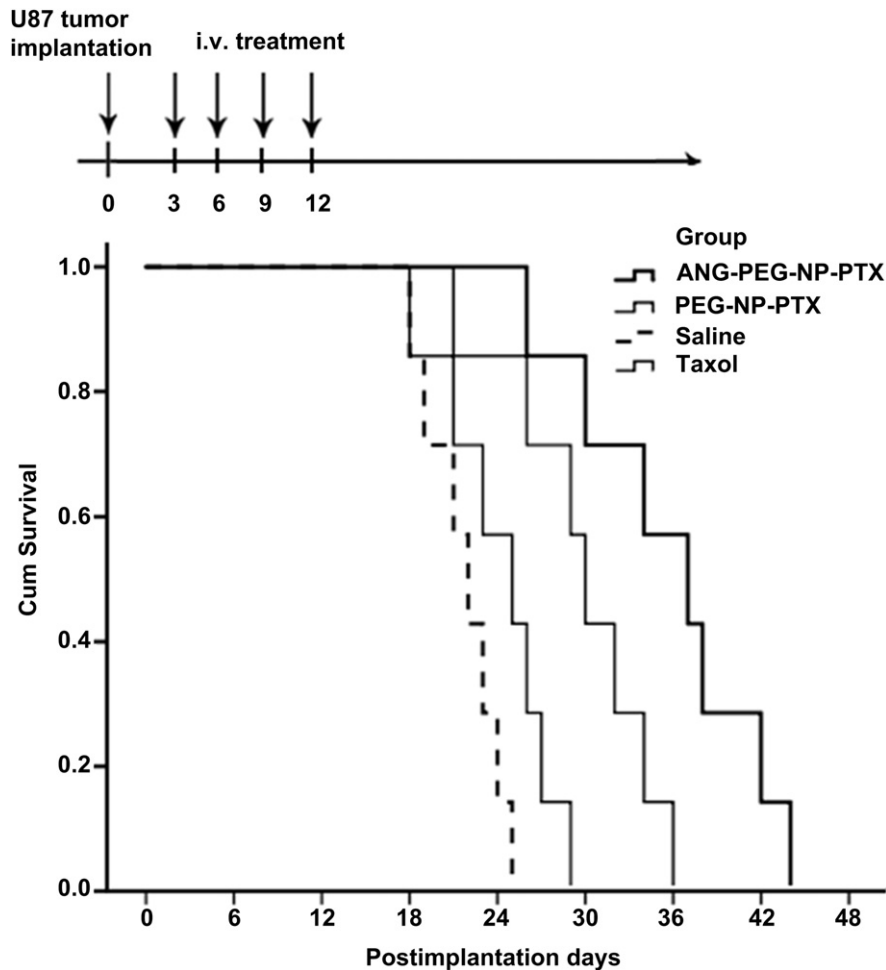
Fig. 7. Kaplan–Meier survival curves of U87 MG glioma-bearing mice treated with different PTX formulations (each dosing 10 mg/kg PTX) at day 3, 6, 9, 12 post implantation ($n = 7$).

respectively. Compared with saline group, the glioma inhibitory ratios of Taxol, PEG-NP-PTX and ANG-PEG-NP-PTX were 20.5%, 36.1% and 65.6%, respectively. Results showed that ANG-PEG-NP-PTX exhibited the strongest inhibitory effect to the glioma tumor volume. As presented in Fig. 6B, it was demonstrated that apoptosis occurred in glioma slices treated with various PTX formulations. It was clear that cell nuclei apoptosis of ANG-PEG-NP-PTX group was more severe as compared to those of Taxol injection and PEG-NP-PTX, suggesting that ANG-PEG-NP could deliver more PTX into glioma tissue and enhance the cellular uptake via LRP mediated endocytosis.

The Kaplan–Meier survival curve of intracranial U87 MG glioma-bearing mice was further investigated to evaluate the *in vivo* anti-glioma efficacy of different PTX formulations. As Fig. 7 and Table 1 presented, the median survival time of ANG-PEG-NP-PTX treatment was 37 days, which was significantly longer than that of mice treated with saline (22 days, $p < 0.01$), Taxol injection (25 days, $p < 0.01$) and PEG-NP-PTX (30 days, $p < 0.05$).

These *in vivo* anti-glioma effects verified that ANG-PEG-NP could improve the chemotherapeutic efficacy of intracranial U87 MG glioma treatment, which was consistent well with the *ex vitro* 3D glioma spheroids experiment. Those findings offered the robust evidence for the Angiopep-2 mediated dual targeting therapeutic benefits of glioma.

3.7. Toxicity evaluation of ANG-PEG-NP

The viability of BCECs and U87 MG cells following 3 days of continuous exposure to Angiopep, blank PEG-NP or blank ANG-PEG-NP at different concentration was measured by MTT assay. As shown in Fig. 8, the Angiopep, blank PEG-NP and blank ANG-PEG-NP preparations were not toxic at concentrations up to 2 mg/mL. The results suggest that ANG-PEG-NP is not inherently toxic to brain capillary endothelial cells and glioma cells probably

Table 1
In vivo effects of PTX formulations on intracranial U87 MG glioma mice model ($n = 7$).

Groups	Dose (mg/kg)	MST[a] (days)	Meidan (days)	Compare with saline[b]	Compare with Taxol[b]	Compare with PEG-NP-PTX[b]
Saline	–	21.7 ± 1.0	22	–	–	–
Taxol	10	24.1 ± 1.4	25	$p > 0.05$	–	–
PEG-NP-PTX	10	29.7 ± 1.9	30	**	*	–
ANG-PEG-NP-PTX	10	35.8 ± 2.4	37	**	**	*

[a] MST: mean survive time.
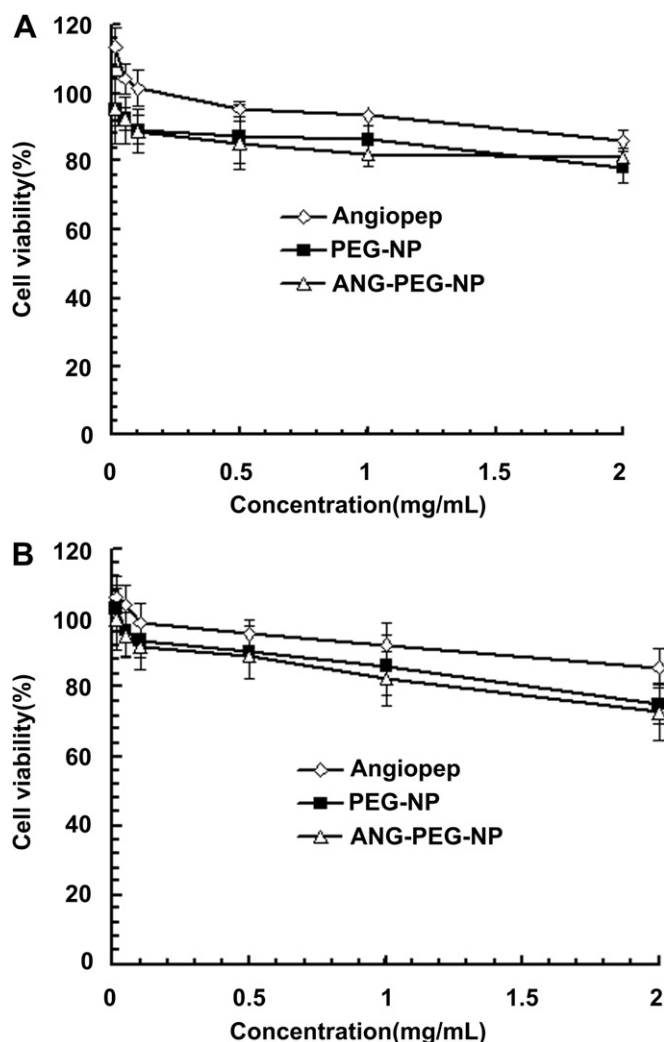[b] **$p < 0.01$, *$p < 0.05$ of log-rank analysis.

Fig. 8. Viability of BCEC (A) and U87 MG (B) cells as a function of varying concentrations of Angiopep and blank nanoparticles (*n* = 3).

due to the non-toxicity of the peptide and biocompatibility of the block polymers.

We further investigated the systemic toxicity of ANG-PEG-NP in mice. Compared with the saline group, following i.v. injection
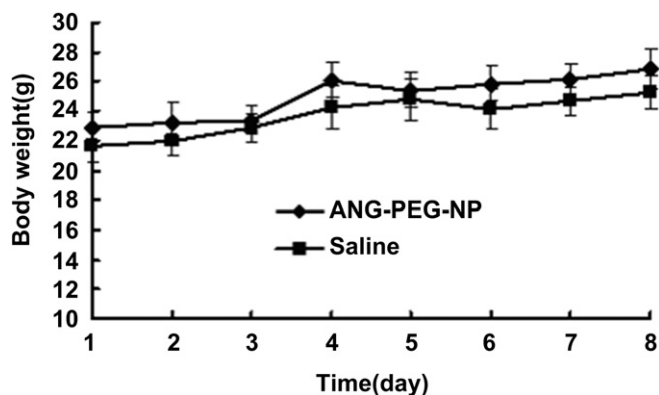

Fig. 9. Change in body weight of mice as a function of time. Mice were injected i.v. with 100 mg/kg blank ANG-PEG-NP or negative control (saline) for 7 days, one dose per day (*n* = 8).

Table 2
Mice blood cell counts after intravenous treatment with ANG-PEG-NP at concentration of 100 mg/kg for 7 days (*n* = 4).

Groups	WBC (10^9/L)	RBC (10^{12}/L)	Platelets (10^9/L)
Saline	4.70 ± 0.90	8.12 ± 0.30	1077 ± 133
ANG-PEG-NP	3.29 ± 1.26	8.10 ± 0.16	954 ± 176

Values are the means ± SD, there was no significant difference of the above parameters between ANG-PEG-NP group and saline control (*p* > 0.05). WBC: white blood cell count; RBC: red blood cell count.

of 100 mg/kg blank ANG-PEG-NP one dose per day for 7 days, no deaths and serious body weight loss were observed in all test groups during the study period (Fig. 9). There was no significant difference in any tested hematological parameters and serum biochemical parameters between the ANG-PEG-NP group and the saline group 24 h after the last administration (Table 2 and Table 3). These results indicated that multiple dosing of ANG-PEG-NP had minimal impact on the function of liver and kidney. To evaluate the acute toxicity of brain caused by ANG-PEG-NP, the tissue sections of cortex, hippocampus, striatum and cerebellum collected 24 h after the last administration were stained with hematoxylin and eosin (H&E). As presented in Fig. 10, the architecture showed no any apparent change in cellular structure and no necrosis, congestion or hydropic degeneration was observed in the cortex, hippocampus, striatum and cerebellum sections as compared to the control group. Results indicated that none visible lesions were observed in the brain of ANG-PEG-NP treatment.

It is well known that most of the intravenously injected nanoparticles are taken up and eliminated by mononuclear phagocyte system (MPS), including liver and kidney tissue [35]. Thus, acute inflammation in liver and kidney caused by ANG-PEG-NP can be characterized by an increase in biochemical parameters including AST, ALT, total bilirubin, blood urea nitrogen and Creatinine, if a non-specific immunoresponse takes place. In our study, no such inflammatory reactions occurred in these tissues. In our previous study, ANG-PEG-NP could enhance penetration into the brain parenchyma through LRP receptor mediated transcytosis process [17]. Therefore, immunohistochemistry of cortex, hippocampus, striatum and cerebellum tissue sections were conducted. Results showed that the toxic effects of ANG-PEG-NP on brain parenchyma were negligible, which was consistent well with the results of *in vitro* cytotoxicity studies. Taken together, our results showed that intravenous successive administration of 100 mg/kg ANG-PEG-NP one dose per day for a week did not cause acute toxicity to the hematological system, liver, kidney and brain parenchyma in mice. Clearly, further work is needed to elucidate the dose–response relationship to acute toxicity. Moreover, the long-term toxic effects of the ANG-PEG-NP are required to investigate in the future study.

Table 3
Mice serum level of biochemical variables after intravenous treatment with ANG-PEG-NP at concentration of 100 mg/kg for 7 days (*n* = 4).

Groups	BUN (mmol/L)	Creatinine (μmol/L)	Total bilirubin (μmol/L)	ALT (U/L)	AST (U/L)
Saline	8.8 ± 1.1	9.3 ± 3.8	1.1 ± 0.12	50.3 ± 14.1	92.8 ± 32.2
ANG-PEG-NP	10.0 ± 1.4	8.8 ± 1.3	1.2 ± 0.42	62.5 ± 18.1	101.6 ± 33.0

Values are the means ± SD, there was no significant difference of the above parameters between ANG-PEG-NP group and saline control (*p* > 0.05). BUN: blood urea nitrogen; ALT, serum alanine aminotransferase; AST: aspartate aminotransferase.
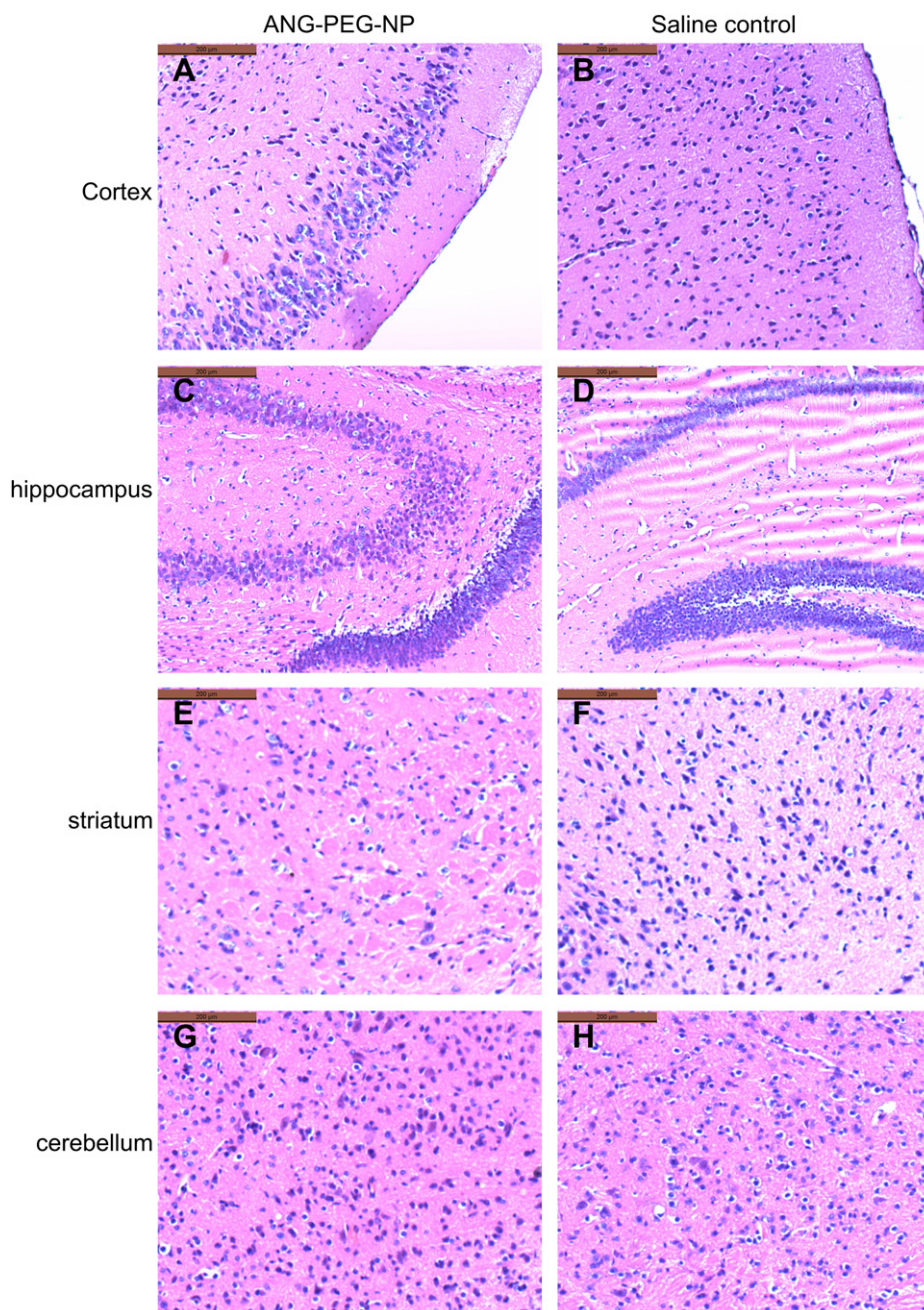
Fig. 10. Histochemistry analysis of cortex (A, B), hippocampus (C, D), striatum (E, F), cerebellum (G, H) section stained with hematoxylin eosin of ICR mice 24 h after i.v. administration of 100 mg/kg ANG-PEG-NP (A, C, E and G) and saline control (B, D, F and H) for 7 days, one dose per day. Bar: 200 μm.

4. Conclusion

We proposed ANG-PEG-NP as a dual targeting drug delivery system for glioma treatment. In this study, we evaluated the availability and safety of ANG-PEG-NP for glioma treatment. The penetration, distribution, and accumulation into 3D glioma tumor spheroid and *in vivo* glioma region of ANG-PEG-NP were much higher than those of plain PEG-NP. The anti-glioblastoma efficacy of ANG-PEG-NP was significantly enhanced in comparison with that of Taxol and PEG-NP. Preliminary safety tests showed no acute toxicity to hematological system, liver, kidney and brain parenchyma in mice after intravenous administration at a dose of 100 mg/kg blank ANG-PEG-NP per day for a week. Our results indicate that Angiopep-conjugated dual targeting PEG-PCL nanoparticle is a potential brain targeting drug delivery system for glioma treatment.

References

[1] Preusser M, de Ribaupierre S, Whörer A, Erridge SC, Hegi M, Weller M, et al. Current concepts and management of glioblastoma. Ann Neurol 2011;70: 9–21.

[2] Ong BY, Ranganath SH, Lee LY. Paclitaxel delivery from PLGA foams for controlled release in post-surgical chemotherapy against glioblastoma multiforme. Biomaterials 2009;30:3189–96.

[3] Liu SH, Guo YB, Huang RQ, Li JF, Huang SY, Kuang YY, et al. Gene and doxorubicin co-delivery system for targeting therapy of glioma. Biomaterials 2012; 33:4907–16.

[4] Pardridge WM. Drug targeting to the brain. Pharm Res 2007;24(9):1733–44.

[5] Chekhonin VP, Baklaushev VP, Yusubalieva GM, Belorusova AE, Gulyaev MV, Tsitrin EB, et al. Targeted delivery of liposomal nanocontainers to the peritumoral zone of glioma by means of monoclonal antibodies against GFAP and the extracellular loop of Cx43. Nanomedicine 2012;8(1):63–70.

[6] Sharpe MA, Marcano DC, Berlin JM, Widmayer MA, Baskin DS, Tour JM. Antibody-targeted nanovectors for the treatment of brain cancers. ACS Nano 2012;6(4):3114–20.

[7] Yan HH, Wang L, Wang JY, Weng XF, Lei H, Wang XX, et al. Two-order targeted brain tumor imaging by using an optical/paramagnetic nanoprobe across the blood brain barrier. ACS Nano 2012;6(1):410–20.

[8] Régina A, Demeule M, Ché C, Lavallée I, Poirier J, Gabathuler R, et al. Antitumor activity of ANG1005, a conjugate between paclitaxel and the new brain delivery vector Angiopep-2. Br J Pharmacol 2008;155:185–97.

[9] Desai A, Vyas T, Amiji M. Cytotoxicity and apoptosis enhancement in brain tumor cells upon coadministration of paclitaxel and ceramide in nanoemulsion formulations. J Pharm Sci 2008;97:2745–56.

[10] Chang SM, Kuhn JG, Robins HI, Schold SC, Spence AM, Berger MS, et al. A Phase II study of paclitaxel in patients with recurrent malignant glioma using different doses depending upon the concomitant use of anticonvulsants: a North American brain tumor consortium report. Cancer 2001;91:417–22.

[11] Postma TJ, Heimans JJ, Luykx SA, van Groeningen CJ, Beenen LF, Hoekstra OS, et al. A phase II study of paclitaxel in chemonaive patients with recurrent high-grade. Ann Oncol 2000;11:409–13.

[12] Ding H, Inoue S, Ljubimov AV, Patil R, Portilla-Arias J, Hu J, et al. Inhibition of brain tumor growth by intravenous poly (beta-L-malic acid) nanobioconjugate with pH-dependent drug release. Proc Natl Acad Sci U S A 2010; 107:18143–8.

[13] Zhan CY, Wei XL, Qian J, Feng LY, Zhu JH, Lu WY. Co-delivery of TRAIL gene enhances the anti-glioblastoma effect of paclitaxel in vitro and in vivo. J Control Release 2012. http://dx.doi.org/10.1016/j.jconrel.2012.02.022.

[14] Du J, Lu WL, Ying X, Liu Y, Du P, Tian W, et al. Dual-targeting topotecan liposomes modified with tamoxifen and wheat germ agglutinin significantly improve drug transport across the blood-brain barrier and survival of brain tumor-bearing animals. Mol Pharm 2009;6(3):905–17.

[15] Li Y, He H, Jia XR, Lu WL, Lou JN, Wei Y. A dual-targeting nanocarrier based on poly(amidoamine) dendrimers conjugated with transferrin and tamoxifen for treating brain gliomas. Biomaterials 2012;33:3899–908.

[16] Gao HL, Qian J, Cao SJ, Yang Z, Pang ZQ, Pan SQ, et al. Precise glioma targeting of and penetration by aptamer and peptide dual-functioned nanoparticles. Biomaterials 2012;33:5115–23.

[17] Xin HL, Jiang XY, Gu JJ, Sha XY, Chen LC, Law k, et al. Angiopep-conjugated poly(ethylene glycol)-co-poly(ε-caprolactone) nanoparticles as dual-targeted drug delivery system for brain glioma. Biomaterials 2011;32:4293–305.

[18] Xin HL, Sha XY, Jiang XY, Chen LC, kitty L, Gu JJ, et al. The brain targeting mechanism of Angiopep-conjugated poly(ethylene glycol)-co-poly(ε-caprolactone) nanoparticles. Biomaterials 2012;33:1673–81.

[19] Huang KY, Ma HL, Liu J, Huo SD, Kumar A, Wei T, et al. Size-dependent localization and penetration of ultrasmall gold nanoparticles in cancer cells, multicellular spheroids, and tumors in vivo. ACS Nano 2012 May 4 [Epub ahead of print].

[20] Xin HL, Chen LC, Gu JJ, Ren XQ, Zhang W, Luo JQ, et al. Enhanced antiglioblastoma efficacy by PTX-loaded PEGylated poly (ε-caprolactone) nanoparticles: in vitro and in vivo evaluation. Int J Pharm 2010;402:238–47.

[21] Tian X, Ying X, Du J, Guo J, Men Y, Zhang Y, et al. Enhanced efficacy of functionalized epirubicin liposomes in treating brain glioma-bearing rats. Eur J Pharm Sci 2010;41(2):232–43.

[22] Ying X, Wen H, Lu WL, Du J, Guo J, Tian W, et al. Dual-targeting daunorubicin liposomes improve the therapeutic efficacy of brain glioma in animals. J Control Release 2010;141:183–92.

[23] Ballangrud A, Yang WH, Dnistrian A, Lampen N, Sgouros G. Growth and characterization of LNCap prostate cancer cell spheroids. Clin Cancer Res 1999;5:3171–6.

[24] Dhanikula RS, Argaw A, Bouchard JF, Hildgen P. Methotrexate loaded polyether-copolyester dendrimers for the treatment of gliomas: enhanced efficacy and intratumoral transport capability. Mol Pharm 2008;5(1):105–16.

[25] Adam JF, Joubert A, Biston JMC, Charvet AM, Peoc'h M, Le Bas JF, et al. Prolonged survival of Fischer rats bearing F98 glioma after iodine-enhanced synchrotron stereotactic radiotherapy. Int J Radiat Oncol Biol Phys 2006;64: 603–11.

[26] Zhu ZS, Li Y, Li XL, Li RT, Jia ZJ, Liu BR, et al. Paclitaxel-loaded poly(N-vinylpyrrolidone)-b-poly(ε-caprolactone) nanoparticles: preparation and antitumor activity in vivo. J Control Release 2010;142:438–46.

[27] Davis ME, Shin DM. Nanoparticle therapeutics: an emerging treatment modality for cancer. Nat Rev Drug Discov 2008;7(9):771–82.

[28] Minchinton A, Tannock I. Drug penetration in solid tumours. Nat Rev Cancer 2006;6:583–92.

[29] Kostarelos K, Emfietzoglou D, Papakostas A, Yang WH, Ballangrud A, Sgouros G. Binding and interstitial penetration of liposomes within avascular tumor spheroids. Int J Cancer 2004;112:713–21.

[30] Desjardins A, Rich J, Quinn J, Vredenburgh J, Gururangan S, Sathornsumetee S, et al. Chemotherapy and novel therapeutic approaches in malignant glioma. Front Biosci 2005;10:2645–68.

[31] De Lange Davies C, Müller H, Hagen I, Garseth M, Hjelstuen MH. Comparison of extracellular matrix in human osteosarcomas and melanomas growing as xenografts, multicellular spheroids, and monolayer cultures. Anticancer Res 1997;17:4317–26.

[32] Ong SM, Zhao Z, Arooz T, Zhao D, Zhang S, Du T, et al. Engineering a scaffold-free 3D tumor model for in vitro drug penetration studies. Biomaterials 2010; 31:1180–90.

[33] Mehta G, Hsiao AY, Ingram M, Luker GD, Takayama S. Opportunities and challenges for use of tumor spheroids as models to test drug delivery and efficacy. J Control Release 2012. http://dx.doi.org/10.1016/j.jconrel.2012.04.045.

[34] Bahmani P, Schellenberger E, Klohs J, Steinbrink J, Cordell R, Zille M, et al. Visualization of cell death in mice with focal cerebral ischemia using fluorescent annexin A5, propidium iodide, and TUNEL staining. J Cereb Blood Flow Metab 2011;31(5):1311–20.

[35] Li SD, Huang L. Pharmacokinetics and biodistribution of nanoparticles. Mol Pharm 2008;5(4):496–504.